Study of the Benzocaine Transfer from Aqueous Solution to the Interior of a Biological Membrane

ARTICLE *in* THE JOURNAL OF PHYSICAL CHEMISTRY B · JULY 2009

Impact Factor: 3.3 · DOI: 10.1021/jp902931s · Source: PubMed

4 AUTHORS, INCLUDING:

Rodolfo D Porasso
Universidad Nacional de San Luis
12 PUBLICATIONS **193** CITATIONS
SEE PROFILE

Jose Javier Lopez Cascales
Universidad Politécnica de Cartagena
62 PUBLICATIONS **778** CITATIONS
SEE PROFILE

Study of the Benzocaine Transfer from Aqueous Solution to the Interior of a Biological Membrane

Rodolfo D. Porasso,[†,‡] W. F. Drew Bennett,[§] S. D. Oliveira-Costa,[‡] and J. J. López Cascales*[,‡]

Instituto de Matemática Aplicada San Luis (IMASL) - Departamento de Física, Universidad Nacional de San Luis/CONICET, D5700HHW, San Luis, Argentina, Department of Biological Sciences, University of Calgary, Calgary AB T3A 2H4, Canada, and Universidad Politécnica de Cartagena, Grupo de Bioinformática y Macromoléculas (BioMac) Aulario II, Campus de Alfonso XIII, 30203 Cartagena, Murcia, Spain

Received: March 31, 2009; Revised Manuscript Received: May 25, 2009

The precise molecular mechanism of general anesthetics remains unknown. It is therefore important to understand where molecules with anesthetic properties localize within biological membranes. We have determined the free energy profile of a benzocaine molecule (BZC) across a biological membrane using molecular dynamics simulation. We use an asymmetric phospholipid bilayer with DPPS in one leaflet of a DPPC bilayer (López Cascales et al. *J. Phys. Chem. B* **2006**, *110*, 2358−2363) to model a biological bilayer. From the free energy profile, we predict the zone of actuation of a benzocaine is located in the hydrocarbon region or at the end of the lipid head, depending of the presence of charged lipids (DPPS) in the leaflet. We observe a moderate increase in the disorder of the membrane and in particular an increase in the disorder of DPPS. Static and dynamic physicochemical properties of the benzocaine, such as its dipole orientation, translational diffusion coefficient, and rotational relaxation time were measured.

1. Introduction

Anesthesia has been a blessing for humanity. In surgery, it provides a reversible loss of consciousness, prevention of any memory of the trauma, muscle relaxation, and pain relief. Local anesthetics have been used clinically for over a century, but the molecular mechanisms by which they alter specific functions of the nervous system remain unclear.[2] Recent investigations implicated a sodium channel as a target for specific, clinically important, local anesthetic effects on mammalian neurons.[3] Benzocaine has been one of the most broadly used local anesthetics via superficial treatment due to its low solubility in aqueous solutions.[4,5] Compared to other local anesthetics, it has a low pK_a, which means it is not hydrolyzed under physiological conditions; i.e., it is always present in its neutral form.[6] Like other molecules with anesthetic properties, benzocaine is thought to follow the Meyer−Overton law[7] by which the anesthetic potency is directly related to its partition coefficient between water and olive oil. However, recently the applicability of this law has been questioned due to two anomalous behaviors. Some molecules that display high partition coefficients do not exhibit anestethic effects. Also, the anesthetic activity is affected by the type of enantiomer used as anesthesia.[2]

Despite all of the molecular information on anesthetics, there is still debate over their location within the interior of a biological membrane. In the past, different experimental[5,6,8−10] and simulation[11−15] studies have been focused on determining the precise location where these anesthetic molecules are located at the interior of the membrane of nervous cells, how this depends on the composition of the phospholipid membrane, and how the structure of the membrane is perturbed by the presence of anesthetics.

We have determined the potential of mean force (PMF) for a benzocaine molecule partitioning from water to the interior of a phospholipid membrane. The PMF provides key thermodynamic properties and information related to barriers and favorable regions to accommodate the benzocaine into the membrane, such as the free energy profile. Molecular dynamics simulations[14,16−18] have emerged as a powerful and precise tool that provides structural and thermodynamics information with atomic detail. We have used a model of an asymmetric phospholipid membrane proposed by Cascales et al.[1] in the attempt of better reproducing a real biological membrane.

The asymmetric membrane resembles the structure of a eukaryotic cell, where charged phosphatidylserines (PSs) are asymmetrically distributed in the cytoplasmic side of the central nervous system, with a PS content in the range 6−20%.[19] In addition to free energy calculations, we have determined the static and dynamical physicochemical properties of benzocaine. We also describe the perturbation of the structure of the membrane due to the presence of benzocaine at its equilibrium position within the membrane.

2. Method and Model

2.1. Setting up the System. To construct the system, we started from a DPPC molecule in which the long molecular axis was oriented perpendicularly to the membrane face (x,y plane). Next, this molecule was randomly rotated and copied 36 times on both sides of the lipid bilayer and water was added to fill in the gaps above and below the phospholipid leaflet, to hydrate the lipid head groups. The asymmetry of lipid distribution was generated by substitution of 12 DPPCs in one of the two leaflets by 12 DPPSs. In addition, 6 DPPCs of the opposite leaflet were removed in order to reproduce the area per lipid of a pure DPPC bilayer, thus avoiding any excess in the surface pressure, such as it was described in detail elsewhere.[1]

Figure 1 shows a snapshot of the periodical system containing 54 DPPC molecules (dipalmitoylphosphatidylcholine), 12 DPPS

* To whom correspondence should be addressed. E-mail: javier.lopez@upct.es.
† Universidad Nacional de San Luis/CONICET.
‡ Universidad Politécnica de Cartagena.
§ University of Calgary.

10.1021/jp902931s CCC: $40.75
Published on Web 06/24/2009

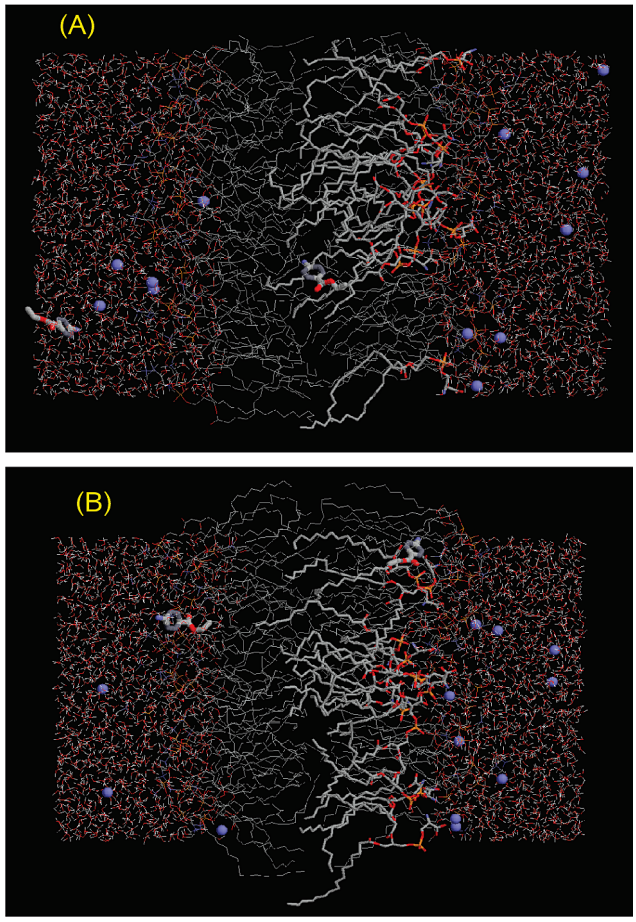

Figure 1. Two snapshots of the system corresponding to simulation 1 (A) and 16 (B) of the batch of 36 simulations carried out in this work. DPPS and benzocaine were plotted with thick sticks, sodium ions with solid beads, and DPPC and water molecules with thin wires.

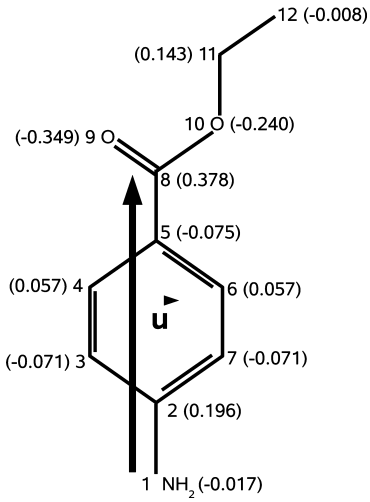

Figure 2. Atomic numeration and charge density of a single benzocaine molecule used in this work.

molecules (dipalmitoylphosphatidylserine), 12 sodium ions (Na^+), 2 benzocaines (BZCs), and 2477 SPCE water molecules.[20] The benzocaine charge distribution, Figure 2, was obtained from semiempirical calculations using the CNDO method[21] implemented in the HyperChem package.[22] The structure of a single benzocaine molecule (BZC) was also generated using the same package mentioned above.

2.2. Simulation Parameters. GROMACS 3.3[23,24] was used to carry out the molecular dynamics simulations. A time step

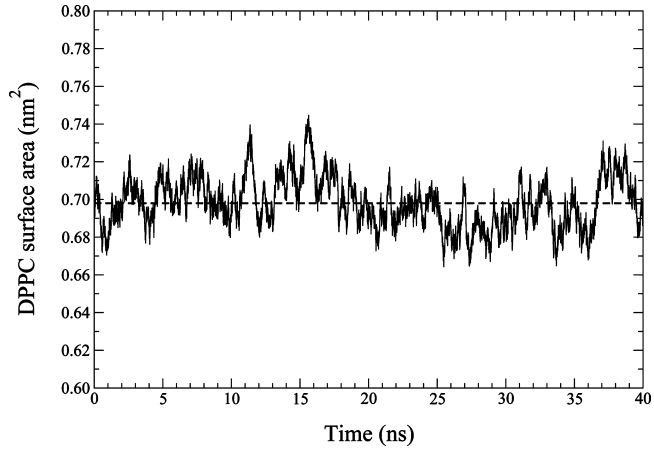

Figure 3. Running DPPC surface area for the leaflet in the absence of DPPS. The horizontal line represents the mean value of the surface area.

of 2 fs was used throughout the simulations. A cutoff of 1 nm was used for calculating the Lennard-Jones interactions. Long range electrostatic interactions were evaluated using the particle mesh Ewald method,[25,26] with the real space interactions calculated using a 0.9 nm cutoff, and the reciprocal space interactions evaluated on a 0.12 nm grid with a fourth-order spline interpolation. A steepest descent energy minimization process was applied to the whole system before running the MD simulations to remove any excess of strain and overlap between neighboring atoms. We have used an NPT thermodynamic ensemble, with a weak temperature and pressure coupling bath algorithm[27] at 350 K and 1 atm, respectively, where a coupling constant of 0.1 and 1 ps was used for temperature and pressure, respectively. The temperature 350 K was the minimum temperature to ensure the system was in the liquid crystalline state (considering that the transition temperatures of DPPC and DPPS are 314 and 326 K, respectively[28,29]).

To confirm that the system achieved an equilibrated state, the time evolution of the surface area per lipid was determined for the DPPC in the membrane leaflet in the absence of DPPS (Figure 3). We observe that the surface area remained constant around 0.69 nm^2 after the first 5 ns of simulation in excellent agreement with the experimental value of 0.70 nm^2 at 350 K for a DPPC bilayer.[30,31]

2.3. Potential of Mean Force (PMF) and Free Energy. The free energy profile of a benzocaine molecule from bulk water to the interior of a lipid bilayer can be calculated as follows:

$$\Delta G_b(z) = -RT \ln \frac{C_b^{eq}(z)}{C_b^*} = -RT \ln(\mathrm{PMF}) \qquad (1)$$

where R is the constant of the gases, T the temperature, $C_b^{eq}(z)$ the equilibrium benzocaine concentration profile at different depths in the interior of the phospholipid membrane, and C_b^* the benzocaine concentration in bulk water. However, if we leave the highly hydrophobic anesthetic molecules to diffuse freely into the phospholipid bilayer, it will provide a poor sampling of its concentration across the membrane during our simulation length, mainly in the zone of the lipid heads with high charge density. To overcome this problem, the umbrella sampling method[32] was used to compute the potential of mean force (PMF) where an artificial biasing potential is added to force the benzocaine to sample the region of interest, in a similar way to that described by MacCallum et al.[33−35] Thus, starting

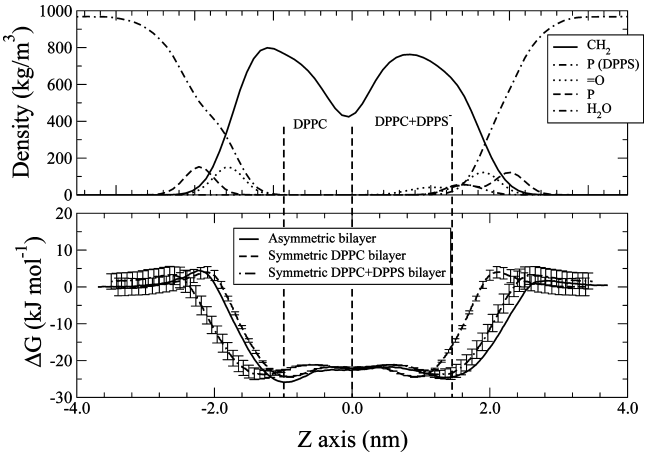

Figure 4. Atomic density and benzocaine free energy profile across the membrane. The error of PMF was estimated from both symmetric parts of the PMF profile.

with the system described in section 2.1, 36 independent simulations of 40 ns each were performed, corresponding to a total simulation time of 1440 ns. In each of the 36 simulations, the benzocaine was restrained at a given depth in the bilayer by a harmonic potential on the z-coordinate perpendicular to the membrane plane only, leaving it to move freely on the x and y axes (two examples of these 36 simulations are depicted in Figure 1). The force constant of this harmonic spring was 3000 kJ·mol^{-1} nm^2 for all of the restrained positions of the benzocaine across the membrane. We have shifted the benzocaine by 0.1 nm in each consecutive simulation window. To save computer time, we calculated the PMF for two benzocaine molecules per simulation. The two benzocaines were always separated by a distance of 3.5 nm along the z axis, such that we asserted the null interaction between both benzocaines. Once these 36 simulations concluded, the weighted histogram analysis method[36] (WHAM) was used to obtain the potential of mean force (PMF) profile across the membrane. Thus, the PMF was calculated from −3.5 to +3.5 nm, where the origin of the Z axis was placed in the center of the membrane.

3. Results and Discussion

3.1. Free Energy (ΔG). Figure 4 depicts the difference of free energy for a benzocaine molecule calculated from bulk water to the interior of the membrane. We set the free energy of benzocaine to zero at $z = -3.5$ nm, which is the free energy in bulk water. From the difference in the value of the free energy in bulk water on the opposite leaflet at $z = 3.5$ nm, we can estimate an error of 0.34 kJ mol^{-1} for the profile.

We observe a clear peak at the lipid/water interface of the DPPC and the DPPC + DPPS monolayers, located at −2.21 and 2.72 nm. From the hight of these peaks, the free energy barrier that benzocaine must cross before penetrating into the membrane is 4.42 and 1.51 kJ mol^{-1} in the absence and presence of DPPS, respectively. The minimum free energy for benzocaine in the bilayer leaflets occurs at z equal to −0.98 and 1.37 nm, with values of −25.9 and −24.6 kJ mol^{-1}, respectively. These values fall within the range of experimental values from 25−30 kJ mol^{-1} measured by Hata et al.[37] for uncharged local anesthetics such as bupivacaine or lidocaine in a DPPC bilayer. For the polar aminoacid Tpr, in a DOPC bilayer, a free energy of −22 kJ/mol was obtained near the lipid head region,[35] in good accordance with our results. The location of the free energy minimum is strongly affected by the asymmetry of the membrane. Thus, for the DPPC leaflet, the minimum clearly matches with the maximum of the methylene groups of the lipid tails. In contrast, for the DPPC + DPPS leaflet, the minimum is shifted toward the region occupied by the carbonyl and phosphorus distribution of the lipids. These results clearly correlate with the experimental results measured by Kuroda et al.[9] from H-NMR spectroscopy. They concluded that, in a DPPC bilayer, benzocaine is located in the core of the tail methylene groups, but in a mixed membrane containing PC (phosphatidylcholine), PS (phosphatidylserine), and PE (phosphatidylethylamine), the benzocaine binding site is located where the acyl chains meet the interfacial polar head groups of the phospholipids.

As a control for our asymmetric model membrane employed in this work, two additional free energy profiles corresponding to benzocaine in a symmetrical DPPC bilayer (36 DPPCs per leaflet) and a symmetrical DPPC + DPPS bilayer (24DPPC + 12DPPS per leaflet) were calculated at 350 K, following the same procedure as that described in section 2.3, with a mean surface area per lipid of 0.69 and 0.58 nm^2, respectively, in a perfect agreement with the values obtained for the leaflets of the asymmetric bilayer in the absence (0.69 nm^2) and presence of DPPS (0.57 nm^2), respectively. From the results depicted in Figure 4, we observe good correlation of both profiles in the leaflet formed only by DPPCs and by the mix of DPPC + DPPS with their respective symmetrical bilayers. The PMF error bar was calculated by considering the values obtained from simulations for both symmetrical leaflets of the bilayers.

From the phosphorus distribution of DPPS in Figure 4, we observe how DPPS occupies the deep inside of the membrane compared with DPPC, and as consequence, a wider head distribution is obtained in the leaflet in the presence of DPPS.

From this thermodynamic data, we are able to calculate the probability of finding a benzocaine molecule in either side of the membrane. In this sense, we will use eq 2:

$$\Delta G = -k_B T \ln k \tag{2}$$

where ΔG is the free energy profile along the z axis, k_B is the Boltzmann constant, T is the temperature, and k is the probability of finding the benzocaine at each position normal to the plane on the bilayer.

The ratio of the probability of finding the benzocaine in one or the other side of the membrane can be calculated as follows:

$$\frac{\int_{-\infty}^{0} \exp[-\Delta G_1/k_B T]}{\int_{0}^{\infty} \exp[-\Delta G_2/k_B T]} = \frac{k_1}{k_2} \tag{3}$$

From the integrals of ΔG, which correspond to both minima, the probability of finding the benzocaine in either leaflet is roughly the same ($k_1/k_2 = 0.92$, 48 vs 52% in the absence or presence of DPPS). With the aim of validating these results, an additional simulation of 50 ns was carried out where both benzocaine molecules were released to move freely. We calculated the mass distribution for both benzocaines across the membrane, and its normalized distribution function was depicted in Figure 5. From the integral of this function from −∞ to 0 and from 0 to +∞, we obtained that the probability of finding the benzocaine was 50.3 and 49.7% for the leaflet in the absence and presence of DPPS, respectively, which corresponds to a ratio of probability of 1.02. In addition, Figure 5 shows how the maximum probability of finding the benzocaine in the

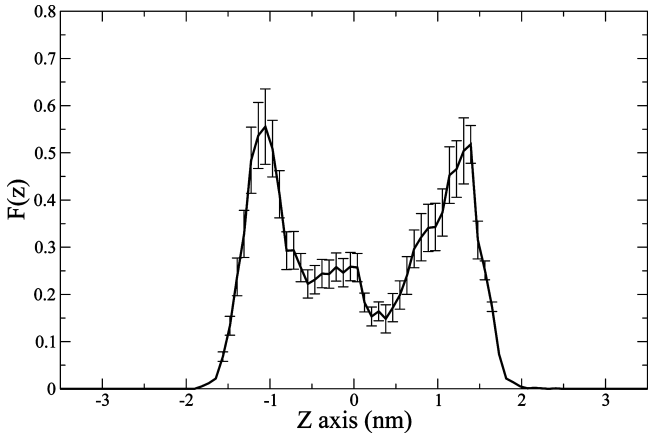

Figure 5. Normalized distribution function of the benzocaine center of mass calculated along 50 ns of simulation across the z axis. The error was calculated after splitting the trajectory into five subtrajectories of 10 ns each.

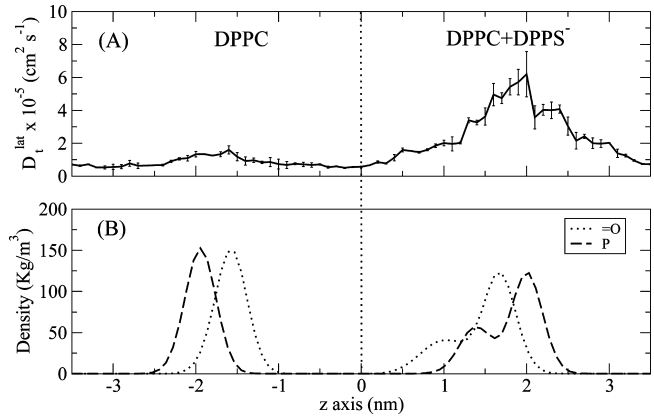

Figure 6. (A) Benzocaine lateral diffusion coefficient from bulk water to the interior of a phospholipid bilayer. The error bars indicate the standard error. (B) Phosphorus and carbonyl moiety density across the lipid bilayer. The error bar was estimated after splitting the trajectory into five subtrajectories of 8 ns each.

interior of the membrane matches with both minima of the free energy, Figure 4.

From the free energy profile ΔG, the partition coefficient of benzocaine between the membrane interior and the aqueous solution can be estimated. Using the minimum in free energy for the DPPC leaflet, we calculate the partition coefficient as follows:

$$K = \exp\left[-\frac{\Delta G_{\min}}{k_B T}\right] \tag{4}$$

Considering a value of $\Delta G_{\min} = -25.9$ kJ mol^{-1} corresponding to this minimum, a partition coefficient of 7044 is obtained. This value agrees with the experimental value of 7200 measured by Hata et al.[37] for uncharged lidocaine in a DPPC bilayer membrane in its liquid crystalline state.

3.2. Translational Diffusion Coefficient. To obtain insight into the physicochemical properties of benzocaine from bulk water to different depths in the membrane, we determined the translational diffusion coefficient of benzocaine. We note that, even when the benzocaine is restrained with respect to the z axis, it retains both degrees of freedom along the x and y axes in the membrane plane. Thus, the lateral diffusion coefficient D_t^{lat} can be calculated from the mean square displacement:

$$\langle x^2 + y^2 \rangle = 4D_t^{lat} t \tag{5}$$

For statistical analysis, the 40 ns trajectory for each umbrella window was split into eight subtrajectories of 5 ns each. We discarded the first subtrajectory to avoid equilibration time, and then, we determined the mean and error. From Figure 6, we observe a plateau in D_t^{lat} at the middle of the phospholipid hydrocarbon region with values that range from 5.4×10^{-6} to 7.0×10^{-6} cm^2 s^{-1}. These values agree with the experimental data of 2.0×10^{-6} cm^2 s^{-1} measured by Rigaud et al.[38] for benzene in egg lecithin films or with simulation data of benzene in DPPC bilayers at 323 K, where Bemporad et al.[39] reported D_t^{lat} in a range from 7.5×10^{-6} to 4.5×10^{-6} cm^2 s^{-1} at the terminal methyl group of the lipid tails and at the carbonyl group between the fatty acid chains and the glycerol fragment, respectively. Also, the results agree with simulation data which range from 0.5×10^{-6} to 2.0×10^{-6} cm^2 s^{-1} for benzene in a DMPC bilayer depending on its position in the interior.[40] On the other hand, we observe a small increase in the phospholipid headgroup region of the leaflet composed only by DPPC, where D_t^{lat} reached a value of 15×10^{-6} cm^2 s^{-1}, which matches with the region of the moiety carbonyl oxygens. For the DPPC + DPPS leaflet, we observe a value of $D_t^{lat} = 61 \times 10^{-6}$ cm^2 s^{-1} near the headgroup region, which is 1 order of magnitude higher than the value attained at the middle of the membrane. This increase in D_t^{lat} at both head regions is strongly related to the low interest of neutral molecules to reside in a region with a high charge density.

Concerning D_t^{lat} in bulk water (corresponding to $Z = \pm 3.5$ nm), values of 7.7×10^{-6} and 7.3×10^{-6} cm^2 s^{-1} emerged from our analysis. These results accord with the value of 10.2×10^{-6} cm^2 s^{-1} measured for benzene in water at 300 K.[41] The slight discrepancy between results is associated with the difference in the hydrodynamic radius between the benzocaine and benzene that might compensate the difference of temperature at which both experiments were carried out.

3.3. Benzocaine Orientation and Reorientational Relaxation Time. The rotational diffusion time of benzocaine at different depths in the membrane provides valuable information related to benzocaine interactions with its environment and the availability of free volume existing in the interior of the membrane. Considering that the benzocaines are restrained at different positions across the membrane by its center of mass, we are able to calculate their rotational properties.

We define a unitary vector $\vec{u}$ from atoms 1 to 8 to estimate different orientational properties of the benzocaine, such as what appears in Figure 2. Thus, from the rotation of unitary vector $\vec{u}$ along the trajectory, the order parameter $\langle P_2(t) \rangle$ can be calculated as follows:

$$\langle P_2(t) \rangle = \langle (3 \cos^2 \theta(t) - 1)/2 \rangle \tag{6}$$

where $\cos \theta(t) = \overrightarrow{u(t)} \cdot \overrightarrow{u(0)}$ describes the orientation of its unitary vector at some initial time $\overrightarrow{u(0)}$ and $\overrightarrow{u(t)}$ is the unitary vector after an elapsed time t. To estimate the error in our calculations, the 40 ns trajectory length was split into eight subtrajectories of 5 ns each, where the first subtrajectory was discarded from analysis. We determined the mean and error from the seven subtrajectories.

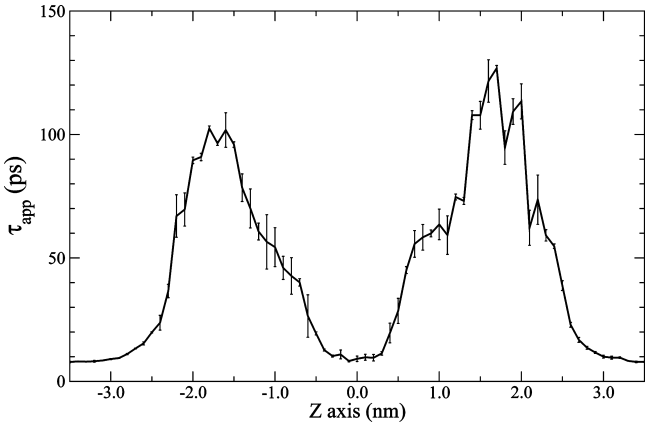

Figure 7. Apparent benzocaine relaxation time τ_{app} from bulk water to the interior of the membrane. Zero was placed in the middle of the phospholipid bilayer. The standard error is indicated with vertical bars. The error bar was estimated after splitting the trajectory into five subtrajectories of 8 ns each.

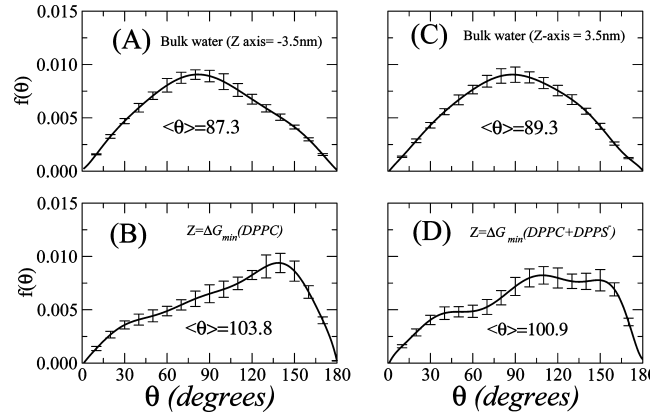

Figure 8. Orientational distribution function of a benzocaine dipole at different positions in the computing box. Parts A and C correspond to bulk water (−3.5 and +3.5 nm), and parts B and D correspond to the minimum of the free energy ΔG at $z = -0.9$ and 1.4 nm, respectively, for the leaflets without and with DPPS, respectively.

To characterize the decays of $\langle P_2(t)\rangle$ with time, in practice, $\langle P_2(t)\rangle$ fits to a multiexponential in the following form:

$$\langle P_2(t)\rangle = \sum_{i=1}^{3} a_i \exp[-t/\tau_i] \tag{7}$$

where τ_i corresponds to the different relaxation times and a_i to the amplitude associated with the time τ_i. Even though the same curve can have different fits, a constant relaxation time τ_{app} can be calculated as follows:

$$\tau_{app} = \frac{\sum_{i=1}^{3} a_i \tau_i}{\sum_{i=1}^{3} a_i} \tag{8}$$

Figure 7 shows the benzocaine relaxation time τ_{app} at different depths in the interior of the membrane. The rotational relaxation time of benzocaine in the middle of the methylene region of the lipid tails was $\tau_{app} = 8.9$ ps. This value agrees with the experimental value of 20 ps reported for di-tert-butyl nitroxide in dipalmitoyllecitin[42] at 323 K, taking into account the different temperatures at which both measurements were carried out. In addition, our results are consistent with the τ value of 5.2 ps obtained for benzyl-alcohol at 325 K in the interior of a DMPC bilayer[11] and the values of τ measured from simulations for benzene in the interior of a DPPC bilayer[39] at 323 K that range from 1 to 12 ps.

When the benzocaine is shifted toward the phospholipid head groups, an increase in the orientational relaxation time is expected. Thus, we observe that τ_{app} increases by 1 order of magnitude up to 102 and 125 ps in the DPPC and DPPC + DPPS, respectively. This increase in τ_{app} is due to the preferred orientations of the benzocaine caused by specific electrostatic interactions between the benzocaine dipole and the membrane environment. This behavior is much more pronounced in the vicinity of the DPPC + DPPS leaflet, as expected from the interactions between the benzocaine dipole and negatively charged DPPS headgroup. Moving out of the membrane, values of τ_{app} of 7.7 and 7.8 ps were measured in bulk water, on both sides of the membrane. This is similar to the value in the middle of the phospholipid membrane. Due to the poor solubility of benzocaine in aqueous solution, to our knowledge, no experimental data of τ_{app} in water have been reported.

From the results presented above, we implicitly assumed preferred orientations of the benzocaine unitary vector $\vec{u}$ as a function of its position at different depths in the membrane. Figure 8 depicts the orientational distribution function of $\vec{u}$ for bulk water and both minima in the free energy (Figure 4). From Figure 8, we observe the same shape for the angular distribution function $f(\theta)$ in bulk water on both sides of the membrane, with mean values of 87.3 and 89.2°, indicating a free orientation of the benzocaine in bulk water. However, in Figure 8B and D, a noticeable difference in the shape of the angular distribution function is observed. The mean values of both distribution functions are quite similar with values of 103.8 and 100.9° for the DPPC and DPPC + DPPS leaflets, respectively. Figure 8D shows three clear peaks at 38, 107, and 150°, denoting three preferred orientations of the benzocaine. Only two maxima at 38 and 140° are observed in Figure 8B, although these are not as pronounced as in the previous case.

3.4. Effect of Benzocaine on the Membrane Structure. To explore the effect of two benzocaine molecules on the membrane structure, two benzocaine molecules were restrained at both Z axis positions corresponding to the minima of the free energy obtained in Figure 4.

We then calculated the deuterium order parameter ($-S_{CD}$) to identify the degree of disorder of the hydrocarbon region inside the membrane. Thus, from simulation, the deuterium order parameter $-S_{CD}$ can be calculated as follows:

$$-S_{CD} = \langle (3\cos^2\theta - 1)/2 \rangle \tag{9}$$

where θ corresponds to the angle formed by the vector that connects the carbons C_{i-1} and C_{i+1} of a phospholipid tail and the z axis normal to the phospholipid interface. The brackets refer to the average that runs over the simulated trajectory. Figure 9 depicts the order parameter of the whole system averaged for both phospholipid tails. We observe that the presence of only one benzocaine positioned at its minimum free energy introduces a slight disorder in the hydrocarbon region. These values are in good agreement with reported experimental data related to the effect of general anesthetics on the structure

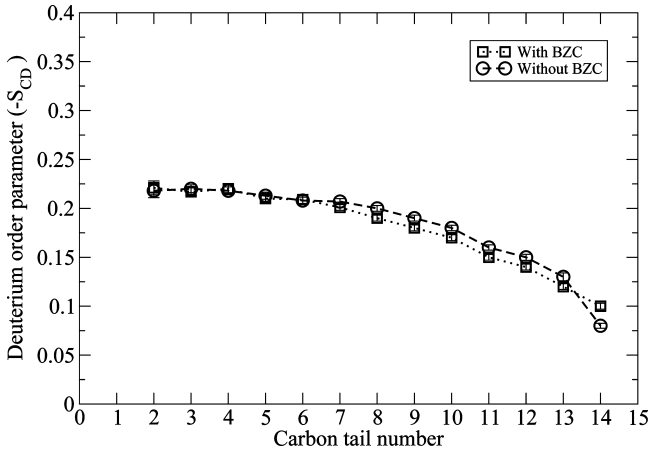

Figure 9. Deuterium order parameter calculated for the whole system, averaged over both phospholipid tails. Carbon number refers to the number of methylene groups of the phospholipid tail. The error bar was calculated after splitting the trajectory into five subtrajectories of 8 ns each.

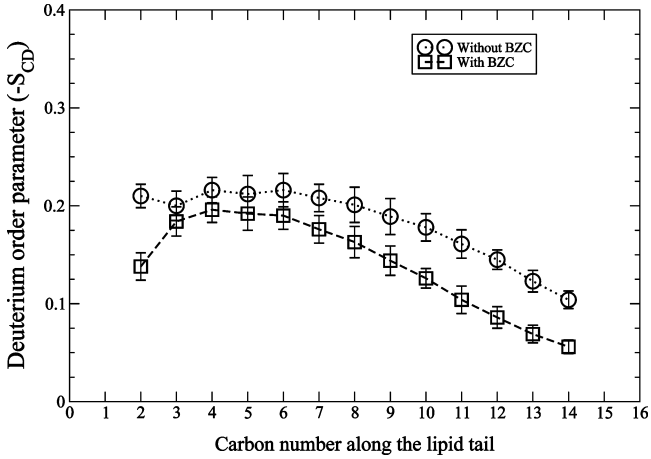

Figure 10. Deuterium order parameter $-S_{CD}$ of $DPPS^-$ averaged over both phospholipid tails. Carbon number refers to the number of methylene groups of the phospholipid tail. The error bar was calculated after splitting the trajectory into five subtrajectories of 8 ns each.

of lipid bilayers studied by X-ray and neutron diffraction techniques[43] or the studies of de Paula et al.[44] by electron paramagnetic resonance (EPR), fluorescence, and H-NMR for uncharged lidocaine in lecithin bilayers. In addition, molecular dynamics simulations provide the ability to analyze the contribution to the order parameter of each of the different lipids that form the membrane. Figure 10 shows how the presence of benzocaine introduces greater disorder in the DPPS conformation, where the bigger error bar found in this case compared to DPPC was only associated to the sample size of the system (considering a ratio of DPPC to DPPS of 4.5:1). From a H-NMR study, Y. Kuroda et al.[9] reported how the presence of benzocaine increased slightly the disorder in the hydrocarbon region of a bilayer composed of PS, PE, and PC in good agreement with our results. From a specific deuterated study, they measured that this disorder is more noticeable beyond carbon 8 of the lipid tails. They also measured that this increase in the disorder of the lipid tails was mainly associated with an increase in the disorder of DPPS, in perfect agreement with our simulation data. These results are of special interest, showing how only two benzocaines positioned at the minimum of the free energy is enough to trigger the behavior described above.

4. Concluding Remarks

Free energy profiles are key thermodynamic properties that provide information about the most probable state of a system. We determined the free energy profile of a benzocaine molecule from bulk water to the interior of a model biological membrane.

From the free energy profile, it was shown that the most probable location of benzocaine, and, in general, neutral molecules with anesthetic properties, depends strongly on the phospholipid composition of the membrane. Thus, in a leaflet formed by pure zwitterionic DPPC, the benzocaine was located in the core of the methylene lipid tail region. In the leaflet composed of DPPC and negatively charged DPPS, the benzocaine is located at the interface between the ends of the lipid heads and the start of the hydrocarbon lipid tails. In addition, from the free energy profile, we were able to estimate that benzocaine resides for a roughly equal time in either leaflet of the membrane. Therefore, the presence of DPPS in one of the membrane leaflets has little effect on the residence time of the benzocaine, although not about its actuation position.

We determined how the presence of only two benzocaine molecules placed in the membrane at both free energy minima increases the disorder of the membrane. There was greater disorder in the negatively charged DPPS lipids compared to the DPPC lipids. Also, the lateral diffusion coefficient D_t^{lat} and the rotational relaxation time of benzocaine increased by almost 1 order of magnitude in the lipid headgroup regions compared with their values in bulk water and in the hydrocarbon core of the membrane. This behavior was strongly affected by the presence of DPPS in one of the membrane leaflets.

Acknowledgment. J.J.L.C. acknowledges the financial support from the Fundacion Seneca de la Region de Murcia, through the project 08647/PPC/08. W.F.D.B. is supported by studentships from NSERC and AHFMR. The authors acknowledge the Computing Center Staff of the Polytechnic University of Cartagena for their support and facilities to carry out the MD simulations on which this paper is based.

References and Notes

(1) López Cascales, J. J.; Otero, T. F.; Smith, B. D.; Gonzalez, C.; Marquez, M. *J. Phys. Chem. B* **2006**, *110*, 2358–2363.
(2) Thompson, S.; Wafford, K. *Curr. Opin. Pharmacol.* **2001**, *1*, 78–83.
(3) Scholz, A. *Br. J. Anaesth.* **2002**, *89*, 52–61.
(4) Butterworth, J. F.; Strichartz, G. R. *Anesthesiology* **1990**, *72*, 711–734.
(5) Matsuki, H.; Hata, T.; Yamanaka, M.; Kaneshima, S. *Colloids Surf., B* **2001**, *22*, 69–76.
(6) Pinto, L. M. A.; Yokaichiya, D. K.; Fraceto, L. F.; de Paula, E. *Biophys. Chem.* **2000**, *87*, 213–223.
(7) Meyer, K. *Trans. Faraday Soc.* **1937**, *33*, 1062–1068.
(8) Turner, G. L.; Oldfield, E. *Nature* **1979**, *277*, 669–700.
(9) Kuroda, Y.; Nasu, H.; Fujiwara, Y.; Nakagawa, T. *J. Membr. Biol.* **2000**, *117*, 117–128.
(10) Shibata, S.; Maeda, K.; Ikema, H.; Ueno, S.; Suezaki, Y.; Liu, S.; Baba, Y.; Ueda, I. *Colloids Surf., B* **2005**, *52*, 197–203.
(11) López Cascales, J.; Hernandez Cifre, J.; Garcia de la Torre, J. *J. Phys. Chem. B* **1998**, *102*, 625–631.
(12) Koubi, L.; Tarek, M.; Bandyopadhyay, S.; Klein, M.; Scharf, D. *Biophys. J.* **2001**, *81*, 3339–3345.
(13) Pasenkiewicz-Gierula, M.; Rog, T.; Grochowski, J.; Serda, P.; Czarnecki, R.; Librowski, T.; Lochynski, S. *Biophys. J.* **2003**, *85*, 1248–1258.
(14) Ahumada, H.; Montecinos, R.; Tieleman, D.; Weiss-López, B. *J. Phys. Chem. A* **2005**, *109*, 6644–6651.
(15) Hogberg, C.; Maliniak, A.; Lyubartsev, A. P. *Biophys. Chem.* **2007**, *125*, 416–424.
(16) van Gunsteren, W. F.; Berendsen, H. J. C. *Angew. Chem., Int. Ed.* **1990**, *29*, 992–1023.
(17) Tieleman, D.; Marrink, S.; Berendsen, H. *Biochim. Biophys. Acta, Biomembr.* **1997**, *1331*, 235–270.

(18) Ekkabut, J.; Baoukina, S.; Triampo, W.; Tang, I.; Tieleman, D.; Monticelli, L. *Nat. Nanotechnol.* **2008**, *3*, 363–368.
(19) Yeagle, P., Ed. *The structure of Biological Membranes*; CRC Press, Inc.: Boca Raton, 1991.
(20) Berendsen, H.; Grigera, J.; Straatsma, T. *J. Phys. Chem.* **1987**, *91*, 6269–6271.
(21) Pople, J. A.; Segal, G. A. *J. Chem. Phys.* **1966**, *44*, 3289.
(22) *HyperChem*; HyperCube, Inc.: Gainesville, 1992.
(23) Lindahl, E.; Hess, B.; van der Spoel, D. *J. Mol. Model.* **2001**, *7*, 306–317.
(24) Berendsen, H.; van der Spoel, D.; van Drunen, R. *Comput. Phys. Commun.* **1995**, *91*, 43–56.
(25) Darden, T.; York, D.; Pedersen, L. *J. Chem. Phys.* **1993**, *98*, 10089–10092.
(26) Essmann, U.; Perea, L.; Berkowitz, M.; Darden, T.; Lee, H.; Pedersen, L. *J. Chem. Phys.* **1995**, *103*, 8577–8593.
(27) Berendsen, H. J. C.; Postma, J. P. M.; van Gunsteren, W. F.; DiNola, A.; Haak, J. R. *J. Chem. Phys.* **1984**, *8*, 3684–3690.
(28) Seeling, A.; Seeling, J. *Biochemistry* **1974**, *13*, 4839–4845.
(29) Cevc, G.; Watts, A.; Marsh, D. *Biochemistry* **1981**, *20*, 4955–4965.
(30) Phillips, M.; Williams, R.; Chapman, D. *Chem. Phys. Lipids* **1969**, *3*, 234–244.
(31) Janiak, M.; Small, D.; Shipley, G. *J. Biol. Chem.* **1979**, *254*, 6068–6078.
(32) Torrie, G.; Valleau, J. *J. Comput. Phys.* **1977**, *23*, 187–199.
(33) MacCallum, J. L.; Tieleman, D. P. *J. Am. Chem. Soc.* **2006**, *128*, 125–130.
(34) Maccallum, J.; Drew Bennett, W.; Tieleman, D. *J. Gen. Physiol.* **2007**, *129*, 371–377.
(35) Maccallum, J.; Drew Bennett, W. F.; Tieleman, D. *Biophys. J.* **2008**, *94*, 3393–3404.
(36) Kumar, S.; Bouzida, D.; Swensen, R.; Kollman, P.; Rosemberg, J. *J. Comput. Chem.* **1992**, *13*, 1011–1021.
(37) Hata, T.; Sakamoto, T.; Matsuki, H.; Kaneshima, S. *Colloids Surf., B* **2000**, *22*, 77–84.
(38) Rigaud, J.; Lange, Y.; Garybobo, C. *Biochim. Biophys. Acta* **1972**, *266*, 72.
(39) Bemporad, D.; Essex, J.; Luttmann, C. *J. Phys. Chem. B* **2004**, *108*, 4875–4884.
(40) Bassolino-Klimas, D.; Alper, H.; Stouch, T. *Biochemistry* **1993**, *32*, 12624–12637.
(41) Lide, D., Ed. *Handbook of Chemistry and Physics*; CRC: Boca Raton, 2002−2003.
(42) Dix, J. A.; Kivelson, D.; Diamond, J. M. *J. Membr. Biol.* **1978**, *40*, 315–342.
(43) Franks, N.; Lieb, W. *J. Mol. Biol.* **1979**, *133*, 469–500.
(44) de Paula, E.; Schreier, S.; Jarrell, H. C.; Fraceto, L. *Biophys. Chem.* **2008**, *132*, 47–54.

JP902931S